RESEARCH ARTICLE

3^2 Factorial Design Approaches for Development, Optimization and Characterization of Artemether Loaded Graphene Oxide Nanocomposites

Harshali Sanjay Jadhav*, Gaurav Jain

Department of IES Institute of Pharmacy, Bhopal, Madhya Pradesh, India

Received: 23rd Feb, 2025; Revised: 17th Apr, 2025; Accepted: 27th May, 2025; Available Online: 25th Apr, 2025

ABSTRACT

Background: Artemether is antimalerial drug having shorter half-life. Conventional form of Artemether required frequent dosing for better pharmacological effect.

Objectives: Recently, graphene oxide-based nano-composition has drawn a lot of attention. The loading of drugs in graphine oxide nanostructure will show delay release behavior.

Methods: In this study, graphene oxide, which was produced using Hummer's technique, loaded with Artemether. The correlation of independence and dependant variables were identified using design of expert software. 3^2 Response surface methodology was engaged to improve formulation. Prepared Artemether loaded graphine oxide nanocomposite were characterized by employing X-ray diffraction (XRD), entrapment efficiency, Differential scanning calorimetry, Fourier transform infrared spectroscopy (FTIR), and drug release.

Results: EE for each of the 13 experiments were from 69.58% to 85.78%. The FTIR spectra indicate the presence of Artemether in graphine oxide nanocomposites. Characteristic endothermic peak of Artemether vanished in thermogram of Artemether in graphine oxide nanocomposites. The crystallinity of Artemether decrease as indicate in the XRD peak. The release profile of the Artemether loaded graphine oxide nanocomposite formulation varied across all batches, ranging from 83.22% to 92.11%.

Conclusion: The developed AM in GO nanocomposites were seem to be favorable approche for sustained drug delivery of Artemether .

Keywords: Artemether, Graphene oxide(GO), 3^2Response Methodology, Delay release; Bioavailability.

How to cite this article: Harshali Sanjay Jadhav, Gaurav Jain. 3^2 Factorial Design Approaches for Development, Optimization and Characterization of Artemether Loaded Graphene Oxide Nanocomposites. International Journal of Drug Delivery Technology. 2025;15(2): 684-92. doi:10.25258/ijddt.15.2.40

Source of support: Nil.

Conflict of interest: None

INTRODUCTION

A significant health and financial burden are caused by malarial parasite infections, especially in less developed nations where they are more common. Malaria is a worldwide health concern despite being curable and preventable[1,2]. Malaria, or disease caused by malarial parasites, is one of the most dangerous public health problems in the world. Malaria kills between 1.5 and 2.7 million public years worldwide, depending on the estimate. One million people die from malaria every year, with three thousand deaths occurring every day[3,4]. They perish as a result of not having access to medical treatment, life-saving medications, and treated bed nets. More than 3000 million cases of malaria occur annually. Last year, there were over five times as many instances of malaria recorded as cases of TB, AIDS, measles, and leprosy combined. Malaria poses a significant threat to more than half of the world's nations. The single-celled protozoan parasite of the genus Plasmodium spreads from an Anopheles mosquito vector to a suitable vertebrate host, which results in malaria[5,6]. The prevention and treatment of malaria employ at least 10 kinds of antimalarial drugs. To eradicate parasites, medications must be used for at least four malarial parasite lifecycles[7,8]. For all antimalarial medications, a 28-day follow-up period is advised. In general, antimalarial medications are advised for the treatment of malaria, contingent upon the severity of the illness[9]. A major concern in treatment of malaria is the increasing level of drug resistance to antimalarials, which may be caused by the ineffectiveness of artemisinin-based monotherapy (chloroquine), since few patients discontinue treatment too soon due to improved symptoms, which is regarded as a positive indicator[10]. Because artemether has fewer adverse effects, is less expensive, and has a greater success rate than other treatments for uncomplicated malaria, the WHO highly recommends using it in combination[11,12]. A semi-synthetic derivative of artemisinin, artemeether is triggered when it complexes with Fe2+ in the parasite Plasmodium ingests. Reactive oxygen species (ROS) and carbon-centered free radicals are formed by artemether as portion of its mode of action, which disrupts the parasite's ability to transfer calcium and carry out other cellular processes. Furthermore, due to its quick removal and shorter half-life of two to three hours, the artemether acts on the malarial parasite instantly[13,14]. The main drawbacks of artemether are its active ingredients' low solubility, bioavailability, and

**Author for Correspondence: harshalijadhav1593@gmail.com*

stability. In order to address the shortcomings of conventional drug delivery methods, novel approaches are favored[15]. These approaches combine the use of cutting-edge technology and more modern dosage forms to increase solubility, bioavailability, and stability of active ingredients while lowering dosage frequency and increasing patient acceptance[16]. As a medicine delivery mechanism based on nanotechnology, graphene oxide has drawn a lot of attention lately. Targeted administration and controlled release of drug, incorporation of hydrophilic and lipophilic drugs, excellent biocompatibility and minimal biotoxicity, and ease of scaling up are only a few of their potential advantages[17,18]. Its large surface area is comparable to that of graphene. Graphene oxide is a commonly utilized pharmacological nanocarrier that has demonstrated compatibility with the human body.

Better drug loading capacity is provided by graphene oxide (GO) because of its two external surfaces[19,20]. In current work, we have synthesized GO by means of an enhanced Hummer's process, and we have loaded athemether onto GO as a drug carrier. Using a statistical approach, the effectiveness of drug encapsulation and release was investigated in relation to different concentrations of Artemether and graphene oxide. Using the 3^2 (three level two factors) response surface approach and Design Expert software, an experimental inquiry was conducted. The shape, encapsulation efficiency, Differential Scanning Calorimetry (DSC), particle size analysis, Fourier transform-infrared (FTIR), X-ray diffractometry, and in vitro drug release of resulting Artemether -loaded GO-nanocomposites were evaluated. For the continuous release of Artemether, the most promising method has been found to be the created Artemether loaded GO-nanocomposites (AM-GO NC).

MATERIALS AND METHODS

Materials

The source of Artemether (AM) was Milan Laboratory in Mumbai, India. We received a free sample of graphite flakes from Rankem Pvt. Ltd. in India. We bought potassium permanganate and hydrogen peroxide from Himedia Pvt. Ltd. in Mumbai, India. Analytical grade chemicals were employed for all other purposes.

Table 1: Formulation composition of nanocomposite of AM loaded GO-NC

Experimental run	Variable			
	Independent		Dependent	
	Artemether X1(mg)	Graphene oxide X2 (mg)	EE Y1(%)	DR Y2 (%)
F1	1	0	73.82	89.68
F2	1	1	79.35	92.02
F3	1	-1	69.2	88.15
F4	0	0	84.36	89.23
F5	0	-1	75.87	85.96
F6	0	0	85.44	90.12
F7	0	0	79.32	83.31
F8	0	0	85.98	91.74
F9	0	1	87.1	87.29
F10	0	0	80.35	87.1
F11	-1	-1	83.15	83.98
F12	-1	1	78.65	86.01
F13	-1	0	81.09	83.22

Coded levels Independent variable	Low (-1)	Medium (0)	High (+1)
X1=Amount of Artemether (AM)	100	150	200
X2=Amount of Graphene oxide	100	150	200

Methods

Synthesis of Graphene Oxide Nanoparticles

In order to produce graphene oxide, the Hummer method was improved. Three grams of graphite flakes, 40 milliliters each of orthophosphoric acid and 360 milliliters of sulfuric acid, and fifteen minutes of stirring were added to the three neck-round bottom flasks. 18 g of KMnO4 were progressively added over the course of 60 minutes, stirring the mixture constantly. Temperature of reaction mixture increased to 35–40°C due to exothermic reaction. Reaction mixture was cooled to ambient temperature and then agitated for a further 12 hours at 45–50°C. To finish the

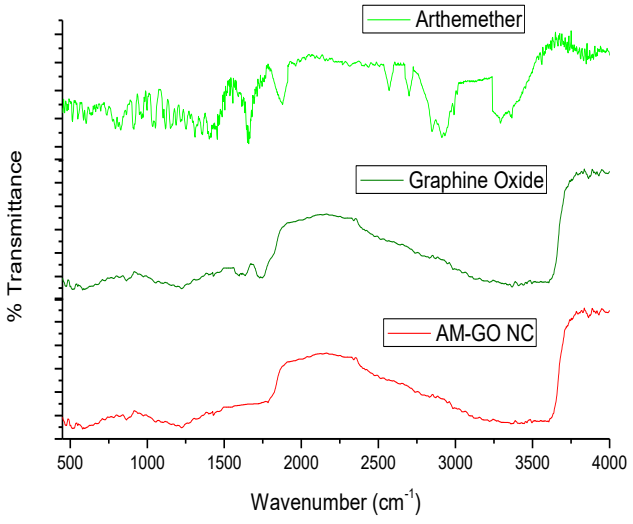

Figure 1: FTIR of AM, GO, and AM loaded GO nanocomposite (AM-GO NC)

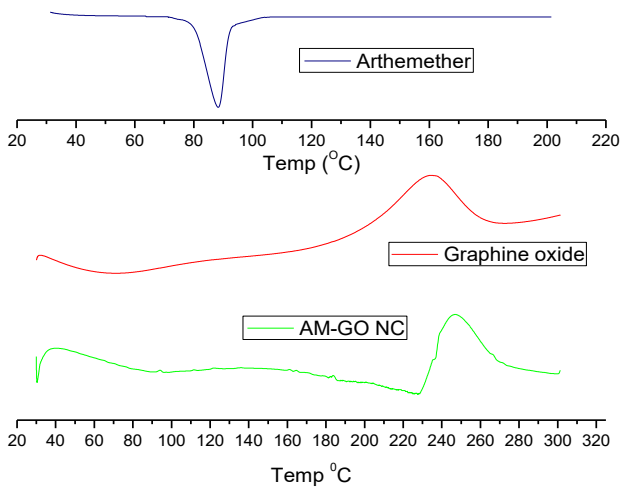

Figure 2: DSC thermograms of pure AM, GO and AM loaded GO nanocomposite (AM-GO NC)

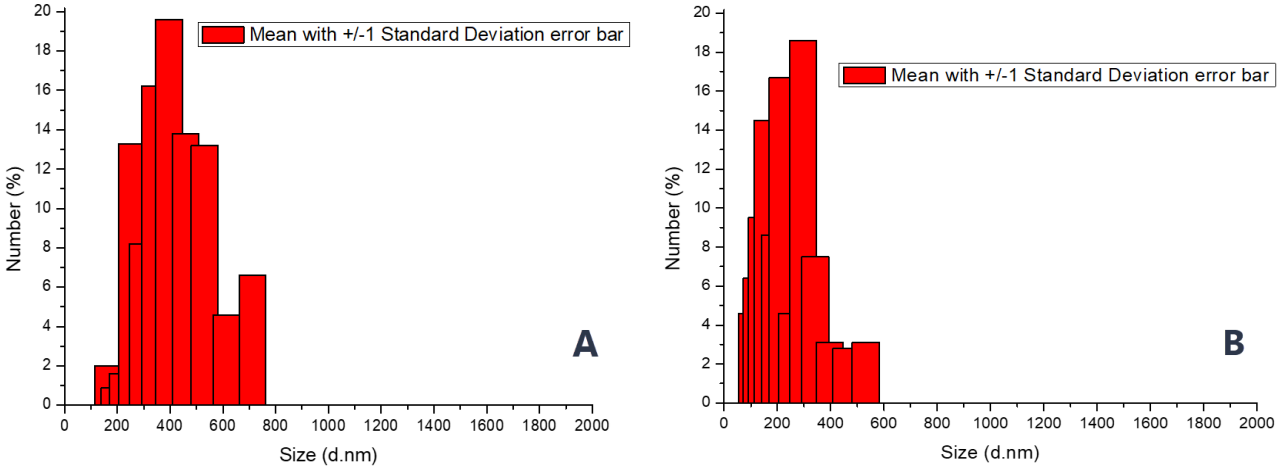

Figure 3: Average size (d. nm) of (a) pure AM (b) AM loaded GO nanocomposite

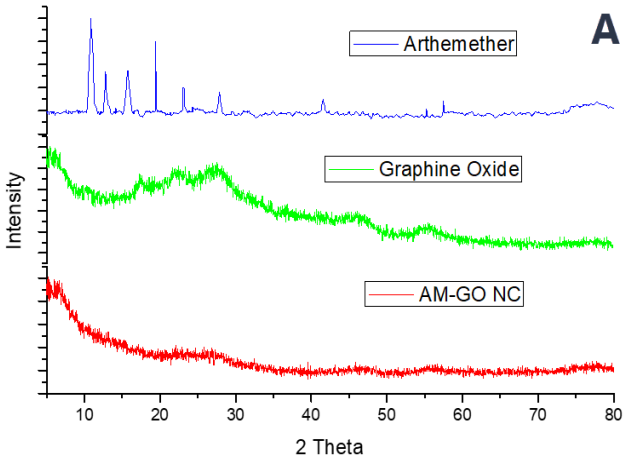

Figure 4: XRD of pure Artemether, GO and Artemether -loaded GO nanocomposite

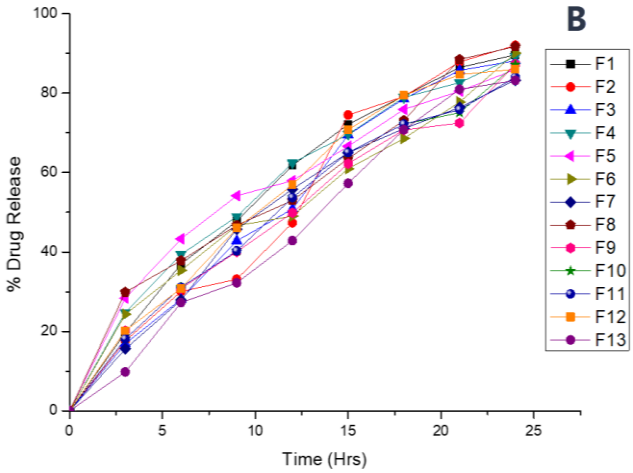

Figure 5: AM and all 13 batches of AM loaded GO nanocomposite of Dissolution profile

reaction, the fluid was progressively added to a beaker that contained 400 g of ice and 3 ml of 30% H_2O_2. Three rinses of 200 ml each of water, 30% HCl, and ethanol were applied to precipitate. Resultant substance was solidified by adding 200 ml of ether. The finished solid product was baked at 60 degrees Celsius 24 hours after being vacuum-dried[21,22].

Development of Artemether -Loaded GO Nanocomposites (AM-GO NC)

The design expert program was used to determine the proper amount of GO, which was then dissolved in 20 milliliters of water and subjected to ultrasonic vibrations for 45 minutes in a bath sonicator. The required amount of Artemether (AM) was dissolved in ethanol, added dropwise, and constantly swirled at room temperature for 6 to 8 hours (see table 1). After that, the mixture was centrifuged for ten minutes. The freeze-dried product was described as the suspension that was produced during the 24-hour lyophilization procedure[23].

Experimental Design for Optimization

The design-expert program was used to carry out statistical experimental inquiry. Influence of independent factors on answers was identified and optimized using 3^2 (three level, two factor) response surface approach. Numerous pilot studies were carried out to increase drug EE and decrease the DR of Artemether -loaded nanocomposites. Early investigations varied the drug and graphene oxide concentrations, as well as the drug release patterns and entrapping efficiency. For these first trial batches, we selected two independent variables: quantity of Artemether (x_1) and amount of graphene oxide (x_2%). Three levels of alteration were applied to these variables: low (1), moderate (0), and high (+1). After 12 hours, dependent variables were determined to be EE (Y_1) and DR (Y_2). Statistical design for a subset of dependent and independent variables is presented in Table 1. To describe impact, following equation was applied.

$$Y = \beta_0 + \beta_1 x_1 + \beta_1 x_1 + \beta_3 x_1 x_2 + \beta_4 x_1^2 + \beta_5 x_2^2 \quad ...(1)$$

Where,

Y is response, β_0 is intercept and $\beta_1 - \beta_5$ is regression coefficients. $x_1, x_2$are individual effects. $x_1 x_2$ is interaction effect and x_1^2, x_2^2 are quadratic effects. Using One-way ANOVA, the significance of model was assessed at $P<0.05$[24,25].

Characterization

Entrapment Efficiency (EE)

The AM-loaded GO nanocomposite was carefully weighed at 10 mg, diluted in 5 ml of DCM, and then mixed with phosphate buffer solution (pH 6.8) to extract AM. Evaporation of an organic solvent was stimulated after 30

Table 2: Kinetic values obtained from different plots of formulations F1 to F13

Time	Batch (F)												
	1	2	3	4	5	6	7	8	9	10	11	12	13
Zero	0.957	0.969	0.977	0.946	0.918	0.967	0.961	0.961	0.977	0.975	0.971	0.960	0.987
First	0.991	0.947	0.976	0.985	0.984	0.885	0.994	0.896	0.925	0.958	0.986	0.984	0.960
Higuchi	0.993	0.946	0.982	0.995	0.994	0.97	0.991	0.956	0.981	0.990	0.992	0.983	0.976
Korsemeyer	0.989	0.961	0.991	0.996	0.993	0.984	0.982	0.962	0.993	0.995	0.994	0.988	0.981

minutes of shaking. The proportion of AM in filtrate was ascertained by UV analysis following proper phosphate buffer dilution. A cuvette with the necessary diluted sample was placed in the UV chamber for examination. Sample was then scanned at maximum wavelength of 225 nm using UV spectrophotometer, and required results were obtained by utilizing the standard. The measurements that were gathered were used to determine the encapsulation efficacy of the pertinent samples[26,27].

$$EE\ (\%) = \frac{Wt.of\ drug\ determined}{Wt.of\ drug\ added} \times 100$$

Drug Loading (% DL)

A 10 mg AM-loaded GO nanocomposite that had been carefully weighed was distributed in DCM before being mixed with phosphate buffer solution (pH 6.7) to facilitate drug extraction. Stirring was kept up until the DCM evaporated. Following dilutions, the dispersion was examined in a UV spectrophotometer (225 nm) and filtered through Whatman paper. An equation based on the absorbance value was used to determine DL[28-30].

$$DR\ (\%) = \frac{Amount\ of\ drug\ determined}{Amount\ of\ drug\ in\ nanocomposites} \times 100$$

Fourier Transforms Infrared Spectroscopy (FTIR)

To ascertain AM-GO compatibility, a Shimadzu FTIR-8400 FTIR spectrophotometer was utilized. KBr pellet technique was used to perform FTIR analyses on GO, AM, and AM loaded GO nanocomposites. In a KBr press, samples and KBr were manually pressed into disk. The range of the individual spectra obtained was 4000–400 cm^{-1}.

Differential Scanning Calorimetry (DSC)

This (DSC-60, Shimadzu) records the thermograms of artemether, AM, and AM loaded GO nanocomposite. Under nitrogen purging, the sample is heated at a rate of 10 °C per minute between 0 and 300 °C.

Particle Size and Polydispersity Index (PDI) Measurements

Zetasizer (Nano ZS, Malvern, UK) was used to measure mean particle diameter and zeta potential of artemether and AM-loaded GO nanocomposite at 25 ºC with distilled water serving as the diluents.

X-ray Diffraction (XRD) Analysis

Using XRD (D8 Advanced, Germany), diffractograms of artemether, GO and AM loaded GO nanocomposites were

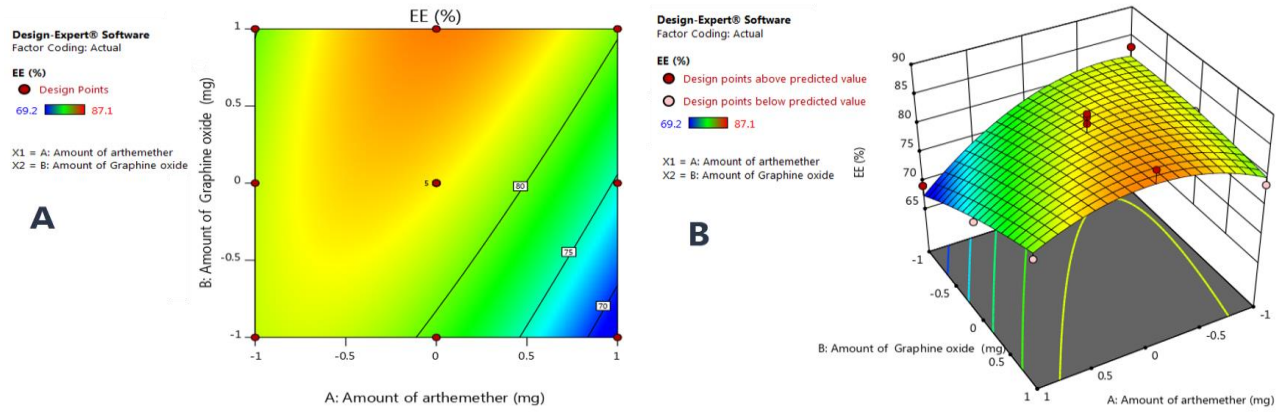

Figure 6: 2D contour plot (a) and 3D response surface plot (b) for entrapment efficiency

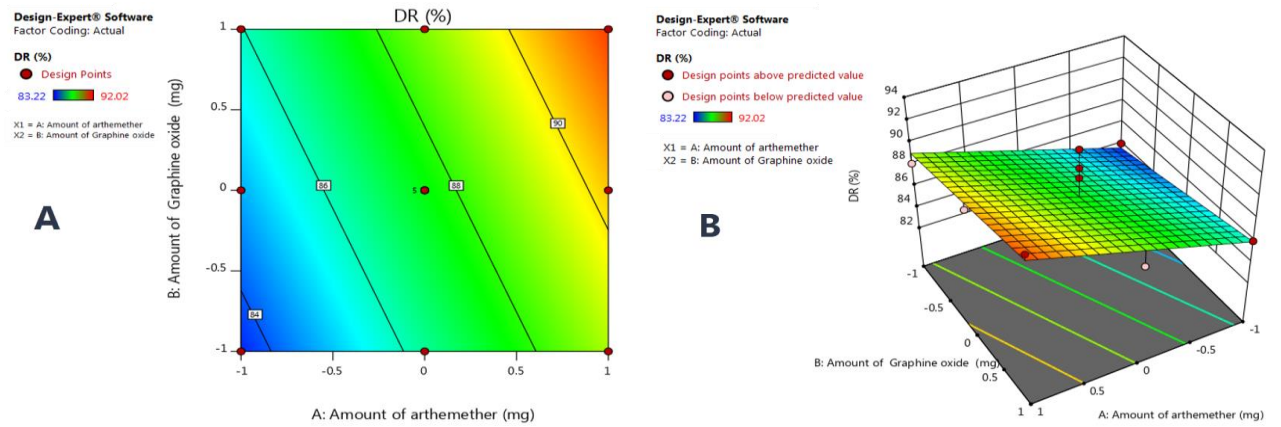

Figure 7: 2D contour plot (a) and 3D response surface plot (b) for drug release

Table 3: Summary of outcomes of regression analysis for responses *Y*1 and *Y*2

Source	Std. Dev.	R^2	Adjusted R^2	Predicted R^2	Press	Remark
Y1 Response						
Linear	4.49	0.3682	0.2419	-0.2863	411.05	
2FI	4.06	0.5361	0.3815	-0.4730	470.71	
Quadratic	3.00	0.8029	0.6622	0.0309	309.68	Suggested
Cubic	2.80	0.8771	0.7049	0.0729	296.26	
Y2 Response						
Linear	2.27	0.5152	0.4182	0.3829	65.72	Suggested
2FI	2.38	0.5231	0.3641	0.3785	66.18	
Quadratic	2.65	0.5387	0.2092	-0.0616	113.05	
Cubic	3.09	0.5528	-0.0733	-5.3339	674.52	

Table 4: ANOVA of models for *Y*1 and *Y*2.

Source	Sum of squares	Df	Mean square	F-value	p-value	Remark
Response Y1						
Model	256.58	5	51.32	5.70	0.0206	significant
x_1	70.18	1	70.18	7.80	0.0268	
x_2	47.49	1	47.49	5.28	0.0552	
x_1x_2	53.66	1	53.66	5.96	0.0446	
x_1^2	63.53	1	63.53	7.06	0.0326	
x_2^2	1.62	1	1.62	0.1802	0.6839	
Response Y2						
Model	54.86	2	27.43	5.31	0.0268	significant
x_1	46.15	1	46.15	8.94	0.0136	
x_2	8.71	1	8.71	1.69	0.2231	

recorded by passing Cu Kα radiation (λ = 1.54 Å) over the samples. A position-sensitive detector was then used to analyze the materials at a 2-theta angle (5-50º)[31-33].

In-vitro Drug Release Studies (DR)

AM-loaded GO nanocomposites with in-vitro active release were processed in a USP Type-I dissolving equipment (100 mesh basket, 100 rpm, 37 ± 0.5 °C) (Electrolab, India). The GO nanocomposites loaded with AM were submerged in 900 milliliters of water containing 1% Polysorbate 80. Aliquots (5 mL) were taken out and replaced with same buffer medium at pre-arranged intervals of 2, 4, 6, 8, and 12 hours. At 210 nm in wavelength, the filtered aliquots were examined using an artemether UV-vis spectrophotometer[34-37].

In Vitro Drug Release Kinetics

Kinetics of drug release from prepared formulation were studied by plotting data from in vitro-drug release studies in three different kinetic models: zero order, which represented cumulative percentage of drug released versus time; first order, which represented log cumulative percentage of drug remaining vs time; and Higuchi's model, which represented cumulative percentage of drug released versus square root of time[38,39].

Stability Studies of AM Loaded GO Nanocomposite

For three months, the AM-loaded GO nanocomposite was kept under extreme conditions in stability chamber with temp of 40 °C and relative humidity of 75%. We examined the morphology, drug content, and release percentage at start and after every month[40,41].

RESULTS AND DISCUSSION

Encapsulation Efficiency (EE) and Drug Loading (DL)

Effects of concentration of Artemether and graphene oxide on factors EE are predicted by 3D counter-plot figure 6b from Design-Expert. Range of EE for each of the 13 studies was 69.58% to 85.78%. The EE was increased when amount of Artemether (X_1) was between 125 to 145 mg and amount of graphene oxide (X_2) was between 175 to 200 mg. Also the DL value was 59.65% - 76.88% for all 13 experiments runs.

Fourier Transform Infrared Spectroscopy (FTIR)

This was completed to identify interaction between drug and excipients. FTIR spectra of pure AM, GO, and AM loaded GO nanocomposite were shown in figure 1. FTIR spectra of artemether (ARTM) indicated occurrence of four characteristic peaks of C–H stretching vibrations at 2698 cm^{-1}, 2813 cm^{-1}, 2906 cm^{-1}, C–H aromatic stretching at 3288 cm^{-1} and C–O–O–C bending vibrations at 1119 cm^{-1}, C–O–C stretching vibrations at 1036 cm^{-1} and 1277.83 cm^{-1}, and C–H bending vibrations at 1452 cm^{-1}[42]. For pure GO, 3662 cm^{-1} for O–H stretching vibrations, 1849 cm^{-1} for C=O stretching vibration, 1721 cm^{-1} for C=C from shows C-C bonds, 1223 cm^{-1} for C–O vibrations, 961 cm^{-1} for epoxy and 779 cm^{-1} for C– O–C. However, in the FTIR spectra AM loaded GO nanocomposite, most of the peaks were resembles to spectra of pure GO, that indicates the presence of AM in GO nanocomposites.

DSC

DSC thermograms of plain GO, AM and AM loaded GO nanocomposite are shown in figure 2. Due to melting point of Artemether, sharp endothermic peak at 87.3ºC was experiential in the thermogram of Artemether [43]. In DSC thermograms of GO, broad endothermic peak is visualized in the range between 40^0C and 80^0C. The subsequent exothermic peak is found in the range between 190- 260^0 C.

Table 5: Statistics on diagnostics cases for different response variables

Run Order	Actual value	Predicted value	Residual	Run Order	Actual value	Predicted value	Residual
	Response Y1				Response Y2		
1	73.82	74.63	-0.8141	1	89.68	90.30	-0.6172
2	84.36	82.85	1.51	2	89.23	87.52	1.71
3	83.15	81.56	1.59	3	83.98	83.55	0.4345
4	79.35	80.34	-0.9938	4	92.02	91.50	0.5178
5	69.20	67.39	1.81	5	88.15	89.09	-0.9422
6	75.87	79.27	-3.40	6	85.96	86.32	-0.3588
7	78.65	79.86	-1.21	7	86.01	85.96	0.0545
8	81.09	81.47	-0.3841	8	83.22	84.75	-1.53
9	85.44	82.85	2.59	9	90.12	87.52	2.60
10	79.32	82.85	-3.53	10	83.31	87.52	-4.21
11	85.98	82.85	3.13	11	91.74	87.52	4.22
12	87.10	84.90	2.20	12	87.29	88.73	-1.44
13	80.35	82.85	-2.50	13	87.10	87.52	-0.4238

Because of the interaction of Artemether and GO as well as the conversion of crystalline form to amorphous form, characteristic endothermic peak of Artemether extinct in thermogram of AM loaded GO nanocomposite

Particle Size Distribution

The mean size of pure AM was about 395.7nm and mean size of optimized batch of AM loaded GO nanocomposite was about 284.2 nm (figure 3a and b).

XRD

The XRD spectra of pure AM, GO and AM loaded GO nanocomposite (AM -GO NC) were shown in figure 4. XRD patterns of Artemether shows $2\emptyset$-scattered angles at10.85°, 12.81°, 14.16°, 15.71°, 17.09°, 19.43°, 23.03°, 27.83° and 41.57°. Peaks in Artemether indicate that it is a crystalline material. The crystalline Artemether peaks in the XRD peak of the Artemether -loaded GO nanocomposite are less intense.

In-vitro Drug Release

Over period of 24 hrs, the release profile of the AM loaded GO nanocomposite formulation varied across all batches, ranging from 83.22% to 92.11%. Every batch of developed AM-loaded GO nanocomposite reveals delayed release action that is sustained for a full day (figure 5). Kinetic models were fixed to release data in order to ascertain DR kinetics. The plot with the highest linearity regression coefficient (R2) was found to be significantly more consistent with Zero order kinetic model for in vitro drug release when compared to other charts. Table 2 listed the medication release method for each batch.

Stability of AM Loaded GO Nanocomposite (AM-GO NC)

An optimized formulation's in vitro dissolving profile, drug content, and physical characteristics were all substantially unaffected.

Optimization

To find effects of independent factors (x_1, x_2.) on dependent variables ($Y1, Y2$), a 3^2 RSM was used. 2D and 3D counter plots were prepared (figures 6a, 7a) to analyse the impacts of an independent variable[44,45]. Artemether concentration (x_1) and graphene oxide concentration (x_2%) were chosen as independent factors, whilst EE (%) and DR (%) were chosen as dependent variables for this study. The EE was predicted to increase when the amounts of Artemether (x_1) and graphene oxide (x_2) were decreased and increased, respectively, by the 2D and 3D plots for EE. However, DR decreased as Artemether (x_1) and graphene oxide (x_2) concentrations increased and decreased, respectively. The EE was between 69.2 % to 85.98 % in all 13 experimental runs, while the DR was between 83.22% - 92.2 %, as shown in table 1. Correlation coefficient (R2) values of 0.8029 and 0.5152, respectively, for quadratic model for the $Y1$and linear equation for $Y2$ indicate a good fit (table 3). The response was identified by following equations for EE ($Y1$) and DR ($Y2$)[46,47].

$$Y1 = +82.85 - 3.42x_1 + 2.81\,x_2 - 4.80\,x_1^2 - 0.7662x_2^2 + 3.66\,x_1x_2 \ldots (3)$$

$$Y2 = +87.52 + 2.77\,x_1 + 1.21x_2 \ldots (4)$$

Table 4 shows ANOVA for models Y1 and Y2 of response. For EE (Y1), quadratic equation indicates that it has $x_1, x_1^2,$ and x_2^2 antagonistic outcome as well as x_2 and x_1x_2. has a synergist effect. In DR (Y2) response, it also signifies linear equation and both factors $i.e$ x_1^2 , x_2^2 have synergist effect. At P<0.05, these independent factors' impacts were statistically significant. F values for each model were 5.70 and 5.31, respectively, and each was significant at P <0.05[48-50]. Together with the actual, predicted, and residual values, Table 5 shows diagnostic case statistics for a number of response variables. Prediction error was ascertained by comparing anticipated value with experimental value that was achieved. Fact that there was minimal variation between the predicted and actual values led to conclusion that the model was strongly fitted[48,51,52].

CONCLUSION

The antimalarial medication artemether has a shorter half-life. For drug delivery graphene oxide-based nano-composition has received a lot of interest. Drug loading in a graphene oxide nanostructure will exhibit delayed release characteristics. 3^2 Response surface approach shows significant correlation between selected factors with their responses. The creation of formulations is aided by the correlations between responses to factors. In all 13 experiments, the EE ranged from 69.58% to 85.78%. FTIR spectrum shows the loading of Artemether in graphine oxide. In the thermogram of the AM-loaded GO nanocomposite, the typical endothermic peak of Artemether vanished. As seen by the XRD peak, Artemether 's

crystallinity is decreasing. The AM loaded GO nanocomposite formulation's release profile varied from 83.22% to 92.11% for 24 hrs duration. From the study we identified that the graphine oxide based nano medicines have good, delayed release showing property. The designed AM in GO nanocomposites appeared to be a potential method for Artemether medication delivery that is maintained.

Abbreviations

AM- Artemether ; AM -GO NC- Artemether loaded graphene oxide nanocomposites; DR- Drug release; DSC- Differential scanning calorimetry; EE- Entrapment Efficiency; FTIR- Fourier transform infrared spectroscopy; GO.graphene oxide; HCl- Hydrochloric acid; K+ - Potassium; NC- Nanocomposites; XRD-X-ray diffraction.

REFERENCES

1. Kogan F, Kogan F, Burden M. Remote Sensing for Malaria: Monitoring and Predicting Malaria from Operational Satellites. Springer International Publishing: Cham. 2020:15-41.
2. Alonso PL, Tanner M. Public health challenges and prospects for malaria control and elimination. Nature Medicine. 2013 Feb;19(2):150-5.
3. Warsame M, Olumese P, Mendis K. Role of medicines in malaria control and elimination. Drug Development Research. 2010 Feb;71(1):4-11.
4. Kokwaro G. Ongoing challenges in the management of malaria. Malaria Journal. 2009 Dec;8(1) (Supplement 1):S2.
5. Wadhwa V, Dutt AK, Akhtar R. The History and Progression of Malaria: A Global and Regional View. Malaria in South Asia: Eradication and Resurgence During the Second Half of the Twentieth Century. 2010:1-27.
6. [6] Björkman A, Bhattarai A. Public health impact of drug-resistant Plasmodium falciparum malaria. Acta Tropica. 2005 Jun 1;94(3):163-9.
7. Patel P, Bagada A, Vadia N. Epidemiology and current trends in malaria Rising Contagious Diseases: Basics, Management, and Treatments. (edited by: SK Amponsah, R Shegokar & YV Pathak). John Wiley & Sons: Chichester. 2024 Mar 11:261-82.
8. Carter R, Mendis KN. Evolutionary and historical aspects of the burden of malaria. Clinical Microbiology Reviews. 2002 Oct;15(4):564-94.
9. Greenwood BM, Fidock DA, Kyle DE, Kappe SH, Alonso PL, Collins FH, Duffy PE. Malaria: progress, perils, and prospects for eradication. The Journal of Clinical Investigation. 2008 Apr 1;118(4):1266-76.
10. Macnab AJ. Global health initiatives to reduce malaria morbidity in school-aged children. GHMJ. 2020 Jun 28;4(1):5-20.
11. Stover KR, King ST, Robinson J. Artemether-lumefantrine: an option for malaria. The Annals of Pharmacotherapy. 2012 Apr;46(4):567-77.
12. Omari AA, Gamble C, Garner P. Artemether-lumefantrine for uncomplicated malaria: a systematic review. Tropical Medicine and International Health. 2004 Feb;9(2):192-9.
13. Esu EB, Effa EE, Opie ON, Meremikwu MM. Artemether for severe malaria. Cochrane Database of Systematic Reviews;2019(6):1-6.
14. Ansari MT, Saify ZS, Sultana N, Ahmad I, Saeed-Ul-Hassan S, Tariq I, Khanum M. Malaria and artemisinin derivatives: an updated review. Mini Reviews in Medicinal Chemistry. 2013 Nov 1;13(13):1879-902.
15. Shirsath NR, Goswami AK. Nanocarriers based novel drug delivery as effective drug delivery: a review. Current Nanomaterials. 2019 Aug 1;4(2):71-83.
16. Patil JS, Naik JB. Carrier based oral nano drug delivery framework: a review. Current Nanomaterials. 2018 Aug 1;3(2):75-85.
17. Liu J, Cui L, Losic D. Graphene and graphene oxide as new nanocarriers for drug delivery applications. Acta Biomaterialia. 2013 Dec 1;9(12):9243-57.
18. Pan Y, Sahoo NG, Li L. The application of graphene oxide in drug delivery. Expert Opinion on Drug Delivery. 2012 Nov 1;9(11):1365-76.
19. Tian L, Pei X, Zeng Y, He R, Li Z, Wang J, Wan Q, Li X. Functionalized nanoscale graphene oxide for high efficient drug delivery of cisplatin. Journal of Nanoparticle Research. 2014 Nov;16(11):1-4.
20. Patil S, Rajkuberan C, Sagadevan S. Recent biomedical advancements in graphene oxide and future perspectives. Journal of Drug Delivery Science and Technology. 2023 Jul 5;86:104737.
21. Deshmukh RV, Paraskar P, Mishra S, Naik J. Development of nateglinide loaded graphene oxide-chitosan nanocomposites: optimization by Box Behnken design. Micro and Nanosystems. 2019 Nov 1;11(2):142-53.
22. Shariare MH, Masum AA, Alshehri S, Alanazi FK, Uddin J, Kazi M. Preparation and optimization of pegylated nano graphene oxide-based delivery system for drugs with different molecular structures using design of experiment (DoE). Molecules. 2021 Mar 7;26(5):1457.
23. Abo-Elseoud WS, Hassan ML, Sabaa MW, Basha M, Hassan EA, Fadel SM. Chitosan nanoparticles/cellulose nanocrystals nanocomposites as a carrier system for the controlled release of repaglinide. International Journal of Biological Macromolecules. 2018 May 1;111:604-13.
24. Shirsath NR, Goswami AK. Design and development of sustained release vildagliptin-loaded silica nanoparticles for enhancing oral bioavailability. BioNanoScience. 2021 Jun;11(2):324-35.
25. Shirsath NR, Goswami AK. Design and development of solid dispersion of valsartan by a lyophilization technique: A 32 factorial design approach. Micro and Nanosystems. 2021 Mar 1;13(1):90-102.
26. Meylina L, Muchtaridi M, Joni IM, Elamin KM, Wathoni N. Hyaluronic acid-coated chitosan nanoparticles as an active targeted carrier of alpha mangostin for breast cancer cells. Polymers. 2023 Feb 18;15(4):1025.

27. Jahanizadeh S, Yazdian F, Marjani A, Omidi M, Rashedi H. Curcumin-loaded chitosan/carboxymethyl starch/montmorillonite bio-nanocomposite for reduction of dental bacterial biofilm formation. International Journal of Biological Macromolecules. 2017 Dec 1;105(1):757-63.
28. Justin R, Chen B. Characterisation and drug release performance of biodegradable chitosan–graphene oxide nanocomposites. Carbohydrate Polymers. 2014 Mar 15;103:70-80.
29. Song MM, Xu HL, Liang JX, Xiang HH, Liu R, Shen YX. Lactoferrin modified graphene oxide iron oxide nanocomposite for glioma-targeted drug delivery. Materials Science and Engineering. C, Materials for Biological Applications. 2017 Aug 1;77:904-11.
30. Ardeshirzadeh B, Anaraki NA, Irani M, Rad LR, Shamshiri S. Controlled release of doxorubicin from electrospun PEO/chitosan/graphene oxide nanocomposite nanofibrous scaffolds. Materials Science and Engineering. C, Materials for Biological Applications. 2015 Mar 1;48:384-90.
31. Deb A, Vimala R. Camptothecin loaded graphene oxide nanoparticle functionalized with polyethylene glycol and folic acid for anticancer drug delivery. Journal of Drug Delivery Science and Technology. 2018 Feb 1;43:333-42.
32. Singh G, Nenavathu BP, Imtiyaz K, Moshahid A Rizvi MM. Fabrication of chlorambucil loaded graphene-oxide nanocarrier and its application for improved antitumor activity. Biomedicine and Pharmacotherapy. 2020 Sep 1;129:110443.
33. Charmi J, Nosrati H, Mostafavi Amjad JM, Mohammadkhani R, Danafar H. Polyethylene glycol (PEG) decorated graphene oxide nanosheets for controlled release curcumin delivery. Heliyon. 2019 Apr 1;5(4):e01466.
34. Abbasi R, Mostafavi Amjad J, Nosrati H, Mohammadkhani R, Danafar H. Synthesis and characterization of pegylated iron and graphene oxide magnetic composite for curcumin delivery. Applied Organometallic Chemistry. 2020 Oct;34(10):e5825.
35. Karami F, Saber-Samandari S. Synthesis and characterization of a novel hydrogel based on carboxymethyl chitosan/sodium alginate with the ability to release simvastatin for chronic wound healing. Biomedical Materials. 2023 Jan 23;18(2):025001.
36. Depan D, Shah J, Misra RD. Controlled release of drug from folate-decorated and graphene mediated drug delivery system: synthesis, loading efficiency, and drug release response. Materials Science and Engineering. 2011 Oct 10;31(7):1305-12.
37. Tao CA, Wang J, Qin S, Lv Y, Long Y, Zhu H, Jiang Z. Fabrication of pH-sensitive graphene oxide–drug supramolecular hydrogels as controlled release systems. Journal of Materials Chemistry. 2012;22(47):24856-61.
38. Singhvi G, Singh M. In-vitro drug release characterization models. Int J Pharm Stud Res. 2011;2(1):77-84.
39. Barzegar-Jalali M, Adibkia K, Valizadeh H, Shadbad MR, Nokhodchi A, Omidi Y, Mohammadi G, Nezhadi SH, Hasan M. Kinetic analysis of drug release from nanoparticles. Journal of Pharmacy and Pharmaceutical Sciences. 2008 May 7;11(1):167-77.
40. Alothman ZA, Rahman N, Siddiqui MR. Review on pharmaceutical impurities, stability studies and degradation products: an analytical approach. Reviews in Advanced Sciences and Engineering. 2013 Jun 1;2(2):155-66.
41. Bajaj S, Singla D, Sakhuja N. Stability testing of pharmaceutical products. Journal of Applied Pharmaceutical Sciences. 2012 Mar 30(Issue):129-38.
42. Ansari MT, Hussain A, Nadeem S, Majeed H, Saeed-Ul-Hassan S, Tariq I, Mahmood Q, Khan AK, Murtaza G. Preparation and characterization of solid dispersions of artemether by freeze-dried method. BioMed Research International. 2015 May 17;2015:109563.
43. Fule RA, Meer TS, Sav AR, Amin PD. Artemether-soluplus hot-melt extrudate solid dispersion systems for solubility and dissolution rate enhancement with amorphous state characteristics. Journal of Pharmaceutics. 2013;2013:151432.
44. Patil P, Khairnar G, Naik J. Preparation and statistical optimization of losartan potassium loaded nanoparticles using Box Behnken factorial design: microreactor precipitation. Chemical Engineering Research and Design. 2015 Dec 1;104:98-109.
45. Pandey S, Patel P, Gupta A. Novel solid lipid nanocarrier of glibenclamide: A factorial design approach with response surface methodology. Current Pharmaceutical Design. 2018 May 1;24(16):1811-20.
46. Saraf A, Dubey N, Dubey N, Sharma M. Box Behnken design based development of curcumin loaded Eudragit S100 nanoparticles for site-spcific delivery in colon cancer. Research Journal of Pharmacy and Technology. 2019;12(8):3672-8.
47. Ashar F, Hani U, Osmani RA, Kazim SM, Selvamuthukumar S. Preparation and optimization of ibrutinib-loaded nanoliposomes using response surface methodology. Polymers. 2022 Sep 17;14(18):3886.
48. Badawi NM, Teaima MH, El-Say KM, Attia DA, El-Nabarawi MA, Elmazar MM. Pomegranate extract-loaded solid lipid nanoparticles: design, optimization, and in vitro cytotoxicity study. International Journal of Nanomedicine. 2018 Mar 6;13:1313-26.
49. Ribeiro AF, de Oliveira Rezende RL, Cabral LM, de Sousa VP. Poly ε-caprolactone nanoparticles loaded with Uncaria tomentosa extract: preparation, characterization, and optimization using the Box–Behnken design. International Journal of Nanomedicine. 2013 Jan 25;8:431-42.
50. Shirsath NR, Goswami AK. Vildagliptin-loaded gellan gum mucoadhesive beads for sustained drug delivery: design, optimisation and evaluation. Materials Technology. 2021 Sep 19;36(11):647-59.
51. Badawi NM, Teaima MH, El-Say KM, Attia DA, El-Nabarawi MA, Elmazar MM. Pomegranate extract-loaded solid lipid nanoparticles: design, optimization, and in vitro cytotoxicity study. International journal of nanomedicine. 2018 Mar 6:1313-26.

52. Zaghloul AA, Mustafa F, Siddiqui A, Khan M. Response surface methodology to obtain β-estradiol biodegradable microspheres for long-term therapy of osteoporosis. Pharmaceutical Development and Technology. 2006 Jan 1;11(3):377-87.

53. Nandy BC, Mazumder B. Formulation and characterizations of delayed release multi-particulates system of indomethacin: optimization by response surface methodology. Current Drug Delivery. 2014 Feb 1;11(1):72-86.